Polarization to Probe an Extra Neutral Gauge Boson at e^+e^- Linear Collider[1]

A. A. Pankov

Department of Physics, Technical University, Gomel, Belarus

Abstract

The sensitivity to the Z' couplings of the processes $e^+e^- \to l^+l^-, \bar{b}b$ and $\bar{c}c$ at the linear collider with $\sqrt{s} = 500\,\mathrm{GeV}$ with initial beam polarization, for typical extended model examples are studied. To this aim, the suitable integrated, polarized, observables directly related to the helicity cross sections that carry information on the individual Z' chiral couplings to fermions are used. We discuss the derivation of separate, model-independent limits on the couplings in the case of no observed indirect Z' signal within the expected experimental accuracy. In the hypothesis that such signals were, indeed, observed we assess the expected accuracy on the numerical determination of such couplings and the consequent range of Z' masses where the individual models can be distinguished from each other as the source of the effect.

[1]Talk given at the International School-Seminar "The Actual Problems of Particle Physics", Gomel, July 30 – August 8, 1999

1 Introduction

Extra neutral gauge bosons are a feature of many models of physics beond the Standard Model (SM). If discovered they would represent irrefutable proof of new physics, most likely that the SM gauge group must be extended [1, 3]. The search for the Z' is included in the physics programme of all the present and future high energy collider facilities. In particular, the strategies for the experimental determination of the Z' couplings to the ordinary SM degrees of freedom, and the relevant discovery limits, have been discussed in the large, and still growing, literature on this subject [1]-[8].

Taking into account the limit $M_{Z'} > 600 - 700\,\mathrm{GeV}$ from 'direct' searches at the Tevatron [9], only 'indirect' (or virtual) manifestations of the Z' can be expected at LEP2 [10] and at the planned e^+e^- linear collider (LC) with CM energy $\sqrt{s} = 500$ GeV [11, 12].

Such effects would be represented by deviations from the calculated SM predictions of the measured observables relevant to the different processes. In this regard, of particular interest for the LC is the annihilation into fermion pairs

$$e^+ + e^- \to \bar{f} + f\,, \tag{1}$$

that gives information on the $Z'ff$ interaction.

In the case of no observed signal within the experimental accuracy, limits on the Z' parameters to a conventionally defined confidence level can be derived, either from a general analysis taking into account the full set of possible Z' couplings to fermions, or in the framework of specific models where characteristic relations among the couplings strongly reduce the number of independent free parameters. Clearly, completely model-independent limits can result only in the optimal situation where the different couplings can be disentangled, by means of suitable observables, and analysed independently so as to avoid potential cancellations. The essential role of the initial electron beam polarization has been repeatedly emphasized in this regard, and the potential of the linear collider along these lines has been extensively reviewed, e.g., in Refs. [7, 8].

The same need of a procedure to disentangle the different Z' couplings arises in the case where deviations from the SM were experimentally observed. Indeed, in this situation, the numerical values of the individual couplings must be extracted from the measured deviations in order to identify the source of these effects and to make tests of the various theoretical

models.

In what follows, we discuss the role of two particular, polarized, variables σ_+ and σ_- in the analysis of the $Z'ff$ interaction from both points of view, namely, the derivation of model-independent limits in the case of no observed deviation and the sensitivity to individual couplings and model identification in the hypothesis of observed deviations.

These observables could directly distinguish the helicity cross sections of process (1) and, therefore, depend on a minimal number of independent free parameters (basically, the product of the Z' chiral couplings to electrons and to the fermionic final state). They have been previously introduced to study Z' effects at LEP2 (no polarization there) [13, 14] and manifestations of four-fermion contact interactions at the LC [15]. Here, we extend the analysis of [13, 14, 16] to the case of the LC with polarized beams. For illustration, we will explicitly consider a specific class of E_6-motivated models and of Left-Right symmetric models.

2 Polarized observables

The polarized differential cross section for process (1) with $f \neq e$, t is given in Born approximation by the s-channel γ, Z and Z' exchanges. Neglecting m_f with respect to the CM energy $\sqrt{s}$, it has the form

$$\frac{d\sigma}{d\cos\theta} = \frac{3}{8}\left[(1+\cos\theta)^2\,\tilde{\sigma}_+ + (1-\cos\theta)^2\,\tilde{\sigma}_-\right], \tag{2}$$

where, in terms of helicity cross sections

$$\tilde{\sigma}_+ = \frac{1}{4}\left[(1+P_e)(1-P_{\bar{e}})\,\sigma_{RR} + (1-P_e)(1+P_{\bar{e}})\,\sigma_{LL}\right], \tag{3}$$

$$\tilde{\sigma}_- = \frac{1}{4}\left[(1+P_e)(1-P_{\bar{e}})\,\sigma_{RL} + (1-P_e)(1+P_{\bar{e}})\,\sigma_{LR}\right], \tag{4}$$

with $(\alpha, \beta = L, R)$

$$\sigma_{\alpha\beta} = N_C\,\sigma_{pt}\,|A_{\alpha\beta}|^2. \tag{5}$$

In these equations, θ is the angle between the initial electron and the outgoing fermion in the CM frame; N_C the QCD factor $N_C \approx 3(1+\frac{\alpha_s}{\pi})$ for quarks and $N_C = 1$ for leptons, respectively; P_e and $P_{\bar{e}}$ are the degrees of longitudinal electron and positron polarization; $\sigma_{\rm pt} \equiv \sigma(e^+e^- \to \gamma^* \to l^+l^-) = (4\pi\alpha^2_{e.m.})/(3s)$; $A_{\alpha\beta}$ are the helicity amplitudes.

According to Eqs. (3) and (4), the cross sections for the different combinations of helicities, that carry the information on the individual $Z'ff$ couplings, can be disentangled *via* the measurement of $\tilde{\sigma}_+$ and $\tilde{\sigma}_-$ with different choices of the initial beams polarization. Instead, the total cross section and the forward-backward asymmetry, defined as:

$$\sigma = \sigma^{\rm F} + \sigma^{\rm B}; \qquad A_{\rm FB} = (\sigma^{\rm F} - \sigma^{\rm B})/\sigma, \tag{6}$$

with $\sigma^{\rm F} = \int_0^1 (d\sigma/d\cos\theta) d\cos\theta$ and $\sigma^{\rm B} = \int_{-1}^0 (d\sigma/d\cos\theta) d\cos\theta$, depend on linear combinations of all helicity cross sections even for longitudinally polarized initial beams. One can notice the relation

$$\tilde{\sigma}_\pm = 0.5\,\sigma\left(1 \pm \frac{4}{3} A_{\rm FB}\right) = \frac{7}{6}\sigma_{\rm F,B} - \frac{1}{6}\sigma_{\rm B,F}. \tag{7}$$

Alternatively, one can directly project out $\tilde{\sigma}_+$ and $\tilde{\sigma}_-$ from Eq. (2), as differences of integrated observables. To this aim, we define $z^* > 0$ such that

$$\left(\int_{-z^*}^{1} - \int_{-1}^{-z^*}\right)(1-\cos\theta)^2\, d\cos\theta = 0. \tag{8}$$

Numerically, $z^* = 2^{2/3} - 1 = 0.59$, corresponding to $\theta^* = 54^\circ$,[2] and for this value of z^*:

$$\left(\int_{-z^*}^{1} - \int_{-1}^{-z^*}\right)(1+\cos\theta)^2\, d\cos\theta = 8\left(2^{2/3} - 2^{1/3}\right). \tag{9}$$

From Eq. (2) one can easily see that the observables

$$\sigma_+ \equiv \sigma_{1+} - \sigma_{2+} = \left(\int_{-z^*}^{1} - \int_{-1}^{-z^*}\right) \frac{d\sigma}{d\cos\theta}\, d\cos\theta, \tag{10}$$

$$\sigma_- \equiv \sigma_{1-} - \sigma_{2-} = \left(\int_{-1}^{z^*} - \int_{z^*}^{1}\right) \frac{d\sigma}{d\cos\theta}\, d\cos\theta \tag{11}$$

are such that

$$\tilde{\sigma}_\pm = \frac{1}{3\,(2^{2/3} - 2^{1/3})}\sigma_\pm = 1.02\,\sigma_\pm. \tag{12}$$

Therefore, for practical purposes one can identify $\sigma_\pm \cong \tilde{\sigma}_\pm$ to a very good approximation. Although the two definitions are practically equivalent

[2] In the case of a reduced angular range $|\cos\theta| < c$, one has $z^* = (1+3c^2)^{1/3} - 1$.

from the mathematical point of view, in the next Section we prefer to use $\sigma_\pm$, that are found more convenient to discuss the expected uncertainties and the corresponding sensitivities to the Z' couplings. Also, it turns out numerically that $z^* = 0.59$ in (10) and (11) maximizes the statistical significance of the results.

The helicity amplitudes $A_{\alpha\beta}$ in Eq. (5) can be written as

$$A_{\alpha\beta} = (Q_e)_\alpha (Q_f)_\beta + g^e_\alpha\, g^f_\beta\, \chi_Z + g'^e_\alpha\, g'^f_\beta\, \chi_{Z'}, \tag{13}$$

in the notation where the general neutral-current interaction is written as

$$-L_{NC} = e J^\mu_\gamma A_\mu + g_Z J^\mu_Z Z_\mu + g_{Z'} J^\mu_{Z'} Z'_\mu. \tag{14}$$

Here, $e = \sqrt{4\pi\alpha_{e.m.}}$; $g_Z = e/s_W c_W$ ($s^2_W = 1 - c^2_W \equiv \sin^2\theta_W$) and $g_{Z'}$ are the Z and Z' gauge couplings, respectively. Moreover, in (13), $\chi_i = s/(s - M^2_i + iM_i\Gamma_i)$ are the gauge boson propagators with $i = Z$ and Z', and the g's are the left- and right-handed fermion couplings. The fermion currents that couple to the neutral gauge boson i are expressed as $J^\mu_i = \sum_f \bar\psi_f \gamma^\mu (L^f_i P_L + R^f_i P_R)\psi_f$, with $P_{L,R} = (1 \mp \gamma_5)/2$ the projectors onto the left- and right-handed fermion helicity states. With these definitions, the SM couplings are

$$R^f_\gamma = Q_f; \qquad L^f_\gamma = Q_f; \qquad R^f_Z = -Q_f s^2_W; \qquad L^f_Z = I^f_{3L} - Q_f s^2_W, \tag{15}$$

where Q_f are fermion electric charges, and the couplings in Eq. (13) are normalized as

$$g^f_L = \frac{g_Z}{e} L^f_Z, \qquad g^f_R = \frac{g_Z}{e} R^f_Z, \qquad g'^f_L = \frac{g_{Z'}}{e} L^f_{Z'}, \qquad g'^f_R = \frac{g_{Z'}}{e} R^f_{Z'}. \tag{16}$$

In what follows, we will limit ourselves to a few representative models predicting new gauge heavy bosons. Specifically, models inspired by GUT inspired scenarios, superstring-motivated ones, and those with Left-Right symmetric origin [4]. These are the χ model occurring in the breaking $SO(10) \to SU(5) \times U(1)_\chi$, the ψ model originating in $E_6 \to SO(10) \times U(1)_\psi$, and the η model which is encountered in superstring-inspired models in which E_6 breaks directly to a rank-5 group. As an example of Left-Right model, we consider the particular value $\kappa = g_R/g_L = 1$, corresponding to the most commonly considered case of Left-Right Symmetric Model (LR). For all such grand-unified E_6 and Left-Right models the Z' gauge coupling in (14) is $g_{Z'} = g_Z s_W$ [4].

As they are constrained from present low-energy data [2] and from recent data from the Tevatron [9], new vector boson effects at the LC are expected to be quite small and therefore should be disentangled from the radiative corrections to the SM Born predictions for the cross section. To this aim, in our numerical analysis we follow the strategy of Refs. [17]-[18], in particular we use the improved Born approximation accounting for the electroweak one-loop corrections.

3 Model independent Z' search and discovery limits

According to Eqs. (3), (4) and (12), by the measurements of σ_+ and σ_- for the different initial electron beam polarizations one determines the cross sections related to definite helicity amplitudes $A_{\alpha\beta}$. From Eq. (13), one can observe that the Z' manifests itself in these amplitudes by the combination of the product of couplings $g'^e_\alpha\, g'^f_\beta$ with the propagator $\chi_{Z'}$. In the situation $\sqrt{s} \ll M_{Z'}$ we shall consider here, only the interference of the SM term with the Z' exchange is important and the deviation of each helicity cross section from the SM prediction is given by

$$\Delta\sigma_{\alpha\beta} \equiv \sigma_{\alpha\beta} - \sigma^{SM}_{\alpha\beta} = N_C\, \sigma_{\rm pt}\, 2\,{\rm Re}\left[\left(Q_e\, Q_f + g^e_\alpha\, g^f_\beta\, \chi_Z\right)\cdot\left(g'^e_\alpha\, g'^f_\beta\, \chi^*_{Z'}\right)\right]. \tag{17}$$

As one can see, $\Delta\sigma_{\alpha\beta}$ depend on the same kind of combination of Z' parameters and, correspondingly, each such combination can be considered as a single 'effective' nonstandard parameter. Therefore, in an analysis of experimental data for $\sigma_{\alpha\beta}$ based on a χ^2 procedure, a one-parameter fit is involved and we may hope to get a slightly improved sensitivity to the Z' with respect to other kinds of observables.

As anticipated, in the case of no observed deviation one can evaluate in a model-independent way the sensitivity of process (1) to the Z' parameters, given the expected experimental accuracy on σ_+ and σ_-. It is convenient to introduce the general parameterization of the Z'-exchange interaction used, e.g., in Refs. [8, 13]:

$$G^f_L = L^f_{Z'}\sqrt{\frac{g^2_{Z'}}{4\pi}\,\frac{M^2_Z}{M^2_{Z'}-s}}, \qquad G^f_R = R^f_{Z'}\sqrt{\frac{g^2_{Z'}}{4\pi}\,\frac{M^2_Z}{M^2_{Z'}-s}}. \tag{18}$$

An advantage of introducing the 'effective' left- and right-handed couplings

of Eq. (18) is that the bounds can be represented on a two-dimensional 'scatter plot', with no need to specify particular values of $M_{Z'}$ or s.

Our χ^2 procedure defines a χ^2 function for any observable $\mathcal{O}$:

$$\chi^2 = \left(\frac{\Delta\mathcal{O}}{\delta\mathcal{O}}\right)^2, \tag{19}$$

where $\Delta\mathcal{O} \equiv \mathcal{O}(Z') - \mathcal{O}(SM)$ and $\delta\mathcal{O}$ is the expected uncertainty on the considered observable combining both statistical and systematic uncertainties. The domain allowed to the Z' parameters by the non-observation of the deviations $\Delta\mathcal{O}$ within the accuracy $\delta\mathcal{O}$ will be assessed by imposing $\chi^2 < \chi^2_{\rm crit}$, where the actual value of $\chi^2_{\rm crit}$ specifies the desired 'confidence' level. The numerical analysis has been performed by means of the program ZEFIT, adapted to the present discussion, which has to be used along with ZFITTER [19], with input values $m_{top} = 175$ GeV and $m_H = 300$ GeV.

In the real case, the longitudinal polarization of the beams will not exactly be ± 1 and, consequently, instead of the pure helicity cross section, the experimentally measured $\sigma_\pm$ will determine the linear combinations on the right hand side of Eqs. (3) and (4) with $|P_e|$ (and $|P_{\bar{e}}|$) less than unity. Thus, ultimately, the separation of σ_{RR} from σ_{LL} will be obtained by solving the linear system of two equations corresponding to the data on σ_+ for, e.g., both signs of the electron longitudinal polarization. The same is true for the separation of σ_{RL} and σ_{LR} using the data on σ_-.

In the 'linear' approximation of Eq. (17), and with $M_{Z'} \gg \sqrt{s}$, the constraints from the condition $\chi^2 < \chi^2_{\rm crit}$ can be directly expressed in terms of the effective couplings (18) as:

$$|G^e_\alpha G^f_\beta| < \frac{\alpha_{e.m.}}{2}\sqrt{\chi^2_{crit}}\left(\frac{\delta\sigma^{SM}_{\alpha\beta}}{\sigma^{SM}_{\alpha\beta}}\right)|A^{SM}_{\alpha\beta}|\frac{M_Z^2}{s}. \tag{20}$$

We need to evaluate the expected uncertainties $\delta\sigma_{\alpha\beta}$. To this aim, starting from the discussion of σ_+, we consider the solutions of the system of four equations corresponding to $P_e = \pm P$ and $P_{\bar{e}} = 0$ in Eqs. (3) and (4):

$$\sigma_{\rm LL} = \frac{1+P}{P}\sigma_+(-P) - \frac{1-P}{P}\sigma_+(P), \tag{21}$$

$$\sigma_{\rm RR} = \frac{1+P}{P}\sigma_+(P) - \frac{1-P}{P}\sigma_+(-P), \tag{22}$$

$$\sigma_{\rm LR} = \frac{1+P}{P}\sigma_-(-P) - \frac{1-P}{P}\sigma_-(P), \tag{23}$$

$$\sigma_{\rm RL} = \frac{1+P}{P}\sigma_-(P) - \frac{1-P}{P}\sigma_-(-P). \tag{24}$$

From these relations, adding the uncertainties, e.g. $\delta\sigma_+(\pm P)$ on $\sigma_+(\pm P)$ in quadrature, $\delta\sigma_{RR}$ has the form

$$\delta\sigma_{RR} = \sqrt{\left(\frac{1+P}{P}\right)^2 (\delta\sigma_+(P))^2 + \left(\frac{1-P}{P}\right)^2 (\delta\sigma_+(-P))^2}, \qquad (25)$$

and $\delta\sigma_{LL}$ can be expressed quite similarly. Also, we combine statistical and systematic uncertainties in quadrature. In this case, if $\sigma_+(\pm P)$ are directly measured *via* the difference (10) of the integrated cross sections $\sigma_{1+}(\pm P)$ and $\sigma_{2+}(\pm P)$, one can see that $\delta\sigma_+^{stat}$ has the simple property: $\delta\sigma_+(\pm P)^{stat} = \left(\sigma^{SM}(\pm P)/\epsilon\mathcal{L}_{int}\right)^{1/2}$, where $\mathcal{L}_{int}$ is the time-integrated luminosity, ϵ is the efficiency for detecting the final state under consideration and $\sigma^{SM}(\pm P)$ is the polarized total cross section. For the systematic uncertainty, we use $\delta\sigma_+(\pm P)^{sys} = \delta^{sys}\left(\sigma_{1+}^2(\pm P) + \sigma_{2+}^2(\pm P)\right)^{1/2}$, assuming that $\sigma_{1+}(\pm P)$ and $\sigma_{2+}(\pm P)$ have the same systematic error δ^{sys}. One can easily see that $\delta\sigma_{LL}$ can be obtained by changing $\delta\sigma_+(P) \leftrightarrow \delta\sigma_+(-P)$ in (25) and that the expression for $\delta\sigma_{RL}$ and $\delta\sigma_{LR}$ also follow from this equation by $\delta\sigma_+ \to \delta\sigma_-$.

Numerically, to exploit Eq. (17) with $\delta\sigma_{\alpha\beta}$ expressed as above, we assume the following values for the expected identification efficiencies and systematic uncertainties on the various fermionic final states [20]: $\epsilon = 100\%$ and $\delta^{sys} = 0.5\%$ for leptons; $\epsilon = 60\%$ and $\delta^{sys} = 1\%$ for b quarks; $\epsilon = 35\%$ and $\delta^{sys} = 1.5\%$ for c quarks. Also, $\chi^2_{crit} = 3.84$ as typical for 95% C.L. with a one-parameter fit. We take $\sqrt{s} = 0.5$ TeV and a one-year run with $\mathcal{L}_{int} = 50\, fb^{-1}$. For for polarized beams, we assume 1/2 of the total integrated luminosity quoted above for each value of the electron polarization, $P_e = \pm P$. Concerning polarization, in the numerical analysis presented below we take three different values, P =1, 0.8 and 0.5, in order to test the dependence of the bounds on this variable.

As already noticed, in the general case where process (1) depends on all four independent $Z'ff$ couplings, only the products $G_R^e G_R^f$ and $G_L^e G_L^f$ can be constrained by the σ_+ measurement *via* Eq. (17), while the products $G_R^e G_L^f$ and $G_L^e G_R^f$ can be analogously bounded by σ_-. The exception is lepton pair production ($f = l$) with ($e - l$) universality of Z' couplings, in which case σ_+ can individually constrain either G_L^e or G_R^e. Also, it is interesting to note that such lepton universality implies $\sigma_{RL} = \sigma_{LR}$ and, accordingly, for $P_{\bar{e}} = 0$ electron polarization drops from Eq. (4) which becomes equivalent to the unpolarized one, with *a priori* no benefit from

Table 1: 95% C.L. model-independent upper limits at LC with $E_{c.m.} = 0.5$ TeV. For polarized beams, we take $\mathcal{L}_{int} = 25\, fb^{-1}$ for each possibility of the electron polarization, $P_e = \pm P$.

couplings		$\lvert G_R^e G_R^f\rvert^{1/2}$ (10^{-3})	$\lvert G_L^e G_L^f\rvert^{1/2}$ (10^{-3})	$\lvert G_R^e G_L^f\rvert^{1/2}$ (10^{-3})	$\lvert G_L^e G_R^f\rvert^{1/2}$ (10^{-3})
observables		σ_{RR}	σ_{LL}	σ_{RL}	σ_{LR}
process	P				
$e^+e^- \to l^+l^-$	1.0	2.1	2.1	3.0	3.2
$e^+e^- \to l^+l^-$	0.8	2.3	2.3	3.3	3.4
$e^+e^- \to l^+l^-$	0.5	2.7	2.7	3.9	4.0
$e^+e^- \to \overline{b}b$	1.0	1.9	2.0	2.5	4.6
$e^+e^- \to \overline{b}b$	0.8	2.2	2.1	2.8	4.8
$e^+e^- \to \overline{b}b$	0.5	3.0	2.3	3.7	5.7
$e^+e^- \to \overline{c}c$	1.0	2.3	2.6	4.1	3.9
$e^+e^- \to \overline{c}c$	0.8	2.5	2.7	4.5	4.1
$e^+e^- \to \overline{c}c$	0.5	3.2	3.0	5.5	4.6

polarization. Nevertheless, the uncertainty in Eq. (25) still depends on the longitudinal polarization P. The 95% C.L. upper bounds on the products of lepton couplings (without assuming lepton universality) are reported in the first three rows of Table 1.

For quark-pair production ($f = c\,, b$), where in general $\sigma_{RL} \neq \sigma_{LR}$ due to the appearance of different fermion couplings, the analysis takes into account the reconstruction efficiencies and the systematic uncertainties previously introduced, and in Table 1 we report the 95% C.L. upper bounds on the relevant products of couplings.

Also, for illustrative purposes, in Fig. 1 we show the 95% C.L. bounds in the plane (G_R^e, G_R^b), represented by the area limited by the four hyperbolas. The shaded region is obtained by combining these limits with the ones derived from the pure leptonic process with lepton universality. Thus, in general we are not able to constrain the individual couplings to a finite region. On the other hand, there would be the possibility of using Fig. 1 to constrain the quark couplings to the Z' to a finite range in the case where some finite effect were observed in the lepton-pair channel. The situation with the other couplings, and/or the c quark, is similar to the

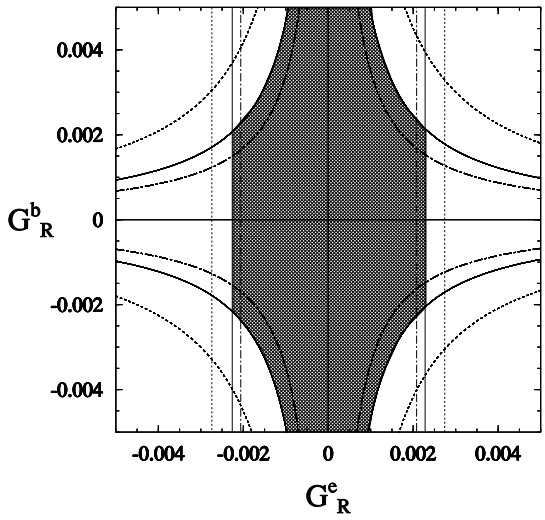

Figure 1: 95% C.L. upper bounds on the model independent Z' couplings in the plane (G^e_R, G^b_R) determined by σ_{RR}. The areas enclosed by vertical straight lines are obtained from the process $e^+e^- \to l^+l^-$, while those enclosed between hyperbolas are from $e^+e^- \to \bar{b}b$ at $\mathcal{L}_{int} = 50$ fb^{-1} and $\sqrt{s} = 500$ GeV. The dot-dash, solid and dotted contours are obtained at $P = 1,\ 0.8,\ 0.5$, respectively. The shaded region is derived from the combination of $e^+e^- \to l^+l^-$ and $e^+e^- \to \bar{b}b$ at $P = 0.8$.

one depicted in Fig. 1.

Table 1 shows that the integrated observables σ_+ and σ_- are quite sensitive to the indirect Z' effects, with upper limits on the relevant products $|G^e_\alpha \cdot G^f_\beta|$ ranging from $2.2 \cdot 10^{-3}$ to $4.8 \cdot 10^{-3}$ at the maximal planned value $P = 0.8$ of the electron longitudinal polarization. In most cases, the best sensitivity occurs for the $\bar{b}b$ final state, while the worst one is for $\bar{c}c$. Decreasing the electron polarization from $P = 1$ to $P = 0.5$ results in worsening the sensitivity by as much as 50%, depending on the final fermion channel.

Regarding the role of the assumed uncertainties on the observables under consideration, in the cases of $e^+e^- \to l^+l^-$ and $e^+e^- \to \bar{b}b$ the

expected statistics are such that the uncertainty turns out to be dominated by the statistical one, and the results are almost insensitive to the value of the systematical uncertainty. Conversely, for $e^+e^- \to \bar{c}c$ both statistical and systematic uncertainties are important. Moreover, as Eqs. (3) and (4) show, a further improvement on the sensitivity to the various Z' couplings in Table 1 would obtain if both initial e^- and e^+ longitudinal polarizations were available [12].

4 Resolving power and model identification

If a Z' is indeed discovered, perhaps at a hadron machine, it becomes interesting to measure as accurately as possible its couplings and mass at the LC, and make tests of the various extended gauge models. To assess the accuracy, the same procedure as in the previous section can be applied to the determination of Z' parameters by simply replacing the SM cross sections in Eqs. (19) and (25) by the ones expected for the 'true' values of the parameters (namely, the extended model ones), and evaluating the χ^2 variation around them in terms of the expected uncertainty on the cross section.

4.1 Z' couplings to leptons

We now examine bounds on the Z' couplings for $M_{Z'}$ fixed at some value. Starting from the leptonic process $e^+e^- \to l^+l^-$, let us assume that a Z' signal is detected by means of the observables σ_+ and σ_-. Using Eqs. (22) and (21), the measurement of σ_+ for the two values $P_e = \pm P$ will allow to extract σ_{RR} and σ_{LL} which, in turn, determine independent and separate values for the right- and left-handed Z' couplings $R^e_{Z'}$ and $L^e_{Z'}$ (we assume lepton universality). The χ^2 procedure determines the accuracy, or the 'resolving power' of such determinations given the expected experimental uncertainty (statistical plus systematic).

In Table 2 we give the resolution on the Z' leptonic couplings for the typical model examples introduced in Section 2, with $M_{Z'} = 1\,\mathrm{TeV}$. In this regard, one should recall that the two-fold ambiguity intrinsic in process (1) does not allow to distinguish the pair of values of $(g'^e_\alpha, g'^f_\beta)$ from the one $(-g'^e_\alpha, -g'^f_\beta)$, see Eq. (17). Thus, the actual sign of the couplings $R^e_{Z'}$ and $L^e_{Z'}$ cannot be determined from the data (in Table 2 we have chosen the signs dictated by the relevant models). In principle, the sign ambiguity of

Table 2: The values of the Z' leptonic and quark chiral couplings for typical models with $M_{Z'} = 1$ TeV and expected 1-σ error bars from combined statistical and systematic uncertainties, as determined at the LC with $E_{c.m.} = 0.5$ TeV and $P = 0.8$.

	χ	ψ	η	LR
$R^e_{Z'}$	$0.204^{+0.042}_{-0.069}$	$-0.264^{+0.052}_{-0.043}$	$-0.333^{+0.038}_{-0.035}$	$-0.438^{+0.029}_{-0.028}$
$L^e_{Z'}$	$0.612^{+0.020}_{-0.020}$	$0.264^{+0.042}_{-0.052}$	$-0.166^{+0.102}_{-0.061}$	$0.326^{+0.036}_{-0.039}$
$R^b_{Z'}$	$-0.612^{+0.110}_{-0.111}$	$-0.264^{+0.111}_{-0.172}$	$0.166^{+0.096}_{-0.075}$	$-0.874^{+0.116}_{-0.138}$
$L^b_{Z'}$	$-0.204^{+0.040}_{-0.042}$	$0.264^{+0.158}_{-0.103}$	$0.333^{+0.230}_{-0.168}$	$-0.110^{+0.080}_{-0.085}$
$R^c_{Z'}$	$0.204^{+0.092}_{-0.090}$	$-0.264^{+0.138}_{-0.207}$	$-0.333^{+0.114}_{-0.145}$	$0.656^{+0.122}_{-0.104}$
$L^c_{Z'}$	$-0.204^{+0.059}_{-0.064}$	$0.264^{+0.222}_{-0.149}$	$0.333^{+0.577}_{-0.326}$	$-0.110^{+0.106}_{-0.134}$

fermionic couplings might be resolved by considering other processes such as, e.g., $e^+e^- \to W^+W^-$.

Another interesting question is the potential of the leptonic process (1) to identify the Z' model underlying the measured signal, through the measurement of the helicity cross sections σ_{RR} and σ_{LL}. Such cross sections only depend on the relevant leptonic chiral coupling and on $M_{Z'}$, so that such resolving power clearly depends on the actual value of the Z' mass. In Figs. 2a and 2b we show this dependence for the E_6 and the LR models of interest here. In these figures, the horizontal lines represent the values of the couplings predicted by the various models, and the lines joining the upper and the lower ends of the vertical bars represent the expected experimental uncertainty at the 95% CL. The intersection of the

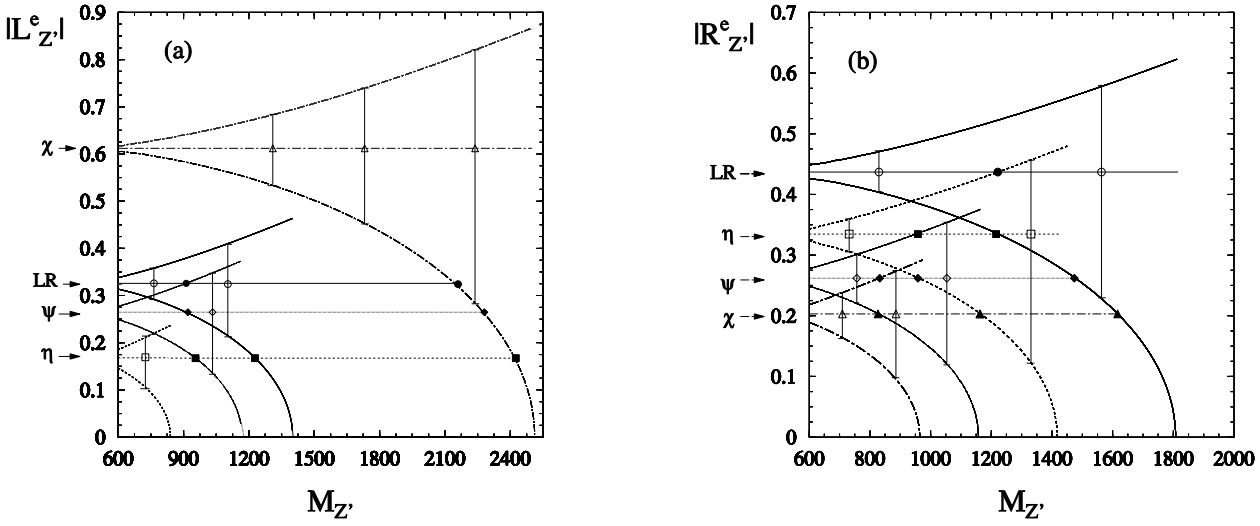

Figure 2: Resolution power at 95% C.L. for the absolute value of the leptonic Z' couplings, $|L^e_{Z'}|$ (a) and $|R^e_{Z'}|$ (b), as a function of $M_{Z'}$, obtained from σ_{LL} and σ_{RR}, respectively, in process $e^+e^- \to l^+l^-$. The error bars combine statistical and systematic uncertainties. Horizontal lines correspond to the values predicted by typical models.

lower such lines with the $M_{Z'}$ axis determines the discovery reach for the corresponding model: larger values of $M_{Z'}$ would determine a Z' signal smaller than the experimental uncertainty and, consequently, statistically invisible. Also, Figs. 2a and 2b show the complementary roles of σ_{LL} and σ_{RR} to set discovery limits: while σ_{LL} is mostly sensitive to the Z'_χ and has the smallest sensitivity to the Z'_η, σ_{RR} provides the best limit for the Z'_{LR} and the worst one for the Z'_χ.

As Figs. 2a and 2b show, the different models can be distinguished by means of $\sigma_\pm$ as long as the uncertainty of the coupling of one model does not overlap with the value predicted by the other model. Thus, the identification power of the leptonic process (1) is determined by the minimum $M_{Z'}$ value at which such 'confusion region' starts. For example, Fig. 2a shows that the χ model cannot be distinguished from the LR, ψ

Table 3: Identification power of process $e^+e^- \to \bar{f}f$ at 95% C.L. expressed in terms of $M_{Z'}$ (in GeV) for typical E_6 and LR models at $E_{c.m.} = 0.5$ TeV and $\mathcal{L}_{int} = 25\, fb^{-1}$ for each value of the electron polarization, $P_e = \pm 0.8$.

	σ_{RR}				σ_{LL}			
$e^+e^- \to l^+l^-$	ψ	η	χ	LR	ψ	η	χ	LR
ψ	—	960	830	1470	—	840	2270	920
η	950	—	970	1210	960	—	2420	1220
χ	830	1165	—	1615	1170	840	—	1400
LR	1160	1220	970	—	915	840	2165	—
$e^+e^- \to bb$	ψ	η	χ	LR	ψ	η	χ	LR
ψ	—	725	1180	2345	—	710	1120	940
η	700	—	1210	2410	750	—	1250	750
χ	1175	1100	—	2130	1130	1140	—	950
LR	1210	1100	1540	—	940	760	1370	—
$e^+e^- \to \bar{c}c$	ψ	η	χ	LR	ψ	η	χ	LR
ψ	—	865	800	1740	—	620	935	800
η	880	—	880	1580	645	—	1035	665
χ	760	1050	—	1840	935	940	—	810
LR	1050	1280	880	—	780	685	1135	—

and η models at Z' masses larger than 2165 GeV, 2270 GeV and 2420 GeV, respectively. The identification power for the typical models are indicated in Figs. 2a and 2b by the symbols circle, diamond, square and triangle. The corresponding $M_{Z'}$ values at 95% C.L. for the typical E_6 and LR models are listed in Table 3, where the Z' models listed in first columns should be distinguished from the ones listed in the first row assumed to be the origin of the observed Z' signal. For this reason Table 3 is not symmetric.

Analogous considerations hold also for σ_{LR} and σ_{RL}. These cross sections give qualitatively similar results for the product $L^e_{Z'}R^e_{Z'}$, but with weaker constraints because of smaller sensitivity.

4.2 Z' couplings to quarks

In the case of process (1) with $\bar{q}q$ pair production (with $q = c,\, b$), the analysis is complicated by the fact that the relevant helicity amplitudes depend on three parameters (g'^e_α, g'^q_β and $M_{Z'}$) instead of two. Nevertheless, there

is still some possibility to derive general information on the Z' chiral couplings to quarks. Firstly, by the numerical procedure introduced above one can determine from the measured cross section the products of electrons and final state quark couplings of the Z', from which one derives allowed regions to such couplings in the independent, two-dimensional, planes $(L^e_{Z'},L^q_{Z'})$ and $(L^e_{Z'},R^q_{Z'})$. The former regions are determined through σ_{LL}, and the latter ones through σ_{LR}. As an illustrative example, in Fig. 3 we depict the bounds from the process $e^+e^- \to \bar{b}b$ in the $(L^e_{Z'},L^b_{Z'})$ and $(L^e_{Z'},R^b_{Z'})$ planes for the Z' of the χ model, with $M_{Z'} = 1\,\mathrm{TeV}$. Taking into account the above mentioned two-fold ambiguity, the allowed regions are the ones included within the two sets of hyperbolic contours in the upper-left and in the lower-right corners of Fig. 3. Then, to get finite regions for the quark couplings, one must combine the hyperbolic regions so obtained with the determinations of the leptonic Z' couplings from the leptonic process (1), represented by the two vertical strips. The corresponding shaded areas represent the determinations of $L^b_{Z'}$, while the hatched areas are the determinations of $R^b_{Z'}$. Notice that, in general, there is the alternative possibility of deriving constraints on quark couplings also in the case of right-handed electrons, namely, from the determinations of the pairs of couplings $(R^e_{Z'},L^b_{Z'})$ and $(R^e_{Z'},R^b_{Z'})$. However, as observed with regard to the previous analysis of the leptonic process, the sensitivity to the right-handed electron coupling turns out to be smaller than for $L^e_{Z'}$, so that the corresponding constraints are weaker.

The determinations of the Z' couplings with the c and b quarks for the typical E_6 and LR models with $M_{Z'} = 1\,\mathrm{TeV}$, are given in Table 2 where the combined statistical and systematic uncertainties are taken into account. Furthermore, similar to the analysis presented in Section 4.1 and the corresponding Figs. 2a and 2b, we depict in Figs. 4a and 4b the different models identification power as a function of $M_{Z'}$, for the reaction $e^+e^- \to \bar{b}b$ as a representative example. The model identification power of the $\bar{b}b$ and $\bar{c}c$ pair production processes are reported in Table 3.

5 Conclusion

We briefly summarize our findings concerning the Z' discovery limits and the models identification power of process (1) *via* the separate measurement of the helicity cross sections $\sigma_{\alpha\beta}$ at the LC, with $\sqrt{s} = 0.5\,\mathrm{TeV}$ and $\mathcal{L}_{int} = 25\,fb^{-1}$ for each value $P_e = \pm P$ the electron longitudinal polarization.

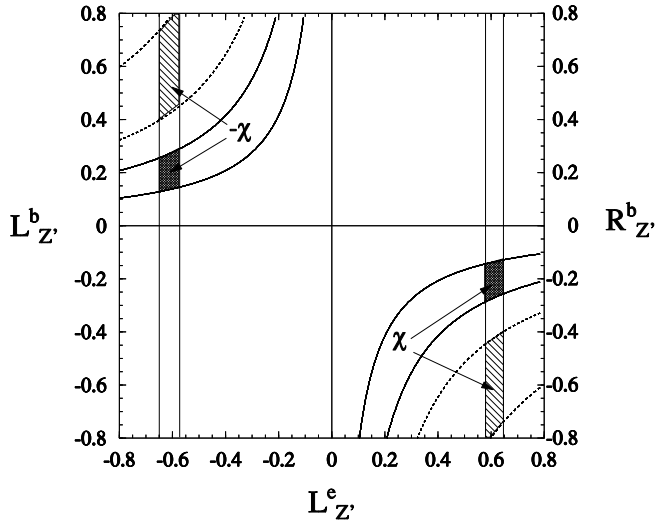

Figure 3: Allowed bounds at 95% C.L. on Z' couplings with $M_{Z'} = 1$ TeV (χ model) in the two-dimension planes ($L^e_{Z'}$,$L^b_{Z'}$) and ($L^e_{Z'}$,$R^b_{Z'}$) obtained from helicity cross sections σ_{LL} (solid lines) and σ_{LR} (dashed lines), respectively. The shaded and hatched regions are derived from the combination of $e^+e^- \to l^+l^-$ and $e^+e^- \to \bar{b}b$ processes. Two allowed regions for each helicity cross section correspond to the two-fold ambiguity discussed in text.

Given the present experimental lower limits on $M_{Z'}$, only indirect effects of the Z' can be studied at the LC. In general, the helicity cross sections allow to extract separate, and model-indpendent, information on the individual 'effective' Z' couplings ($G^e_\alpha \cdot G^f_\beta$). As depending on the minimal number of free parameters, they may be expected to show some convenience with respect to other observables in an analysis of the experimental data based on a χ^2 procedure.

In the case of no observed signal, i.e., no deviation of $\sigma_{\alpha\beta}$ from the SM prediction within the experimental accuracy, one can directly obtain model-independent bounds on the leptonic chiral couplings of the Z' from $e^+e^- \to l^+l^-$ and on the products of couplings $G^e_\alpha \cdot G^q_\beta$ from $e^+e^- \to \bar{q}q$

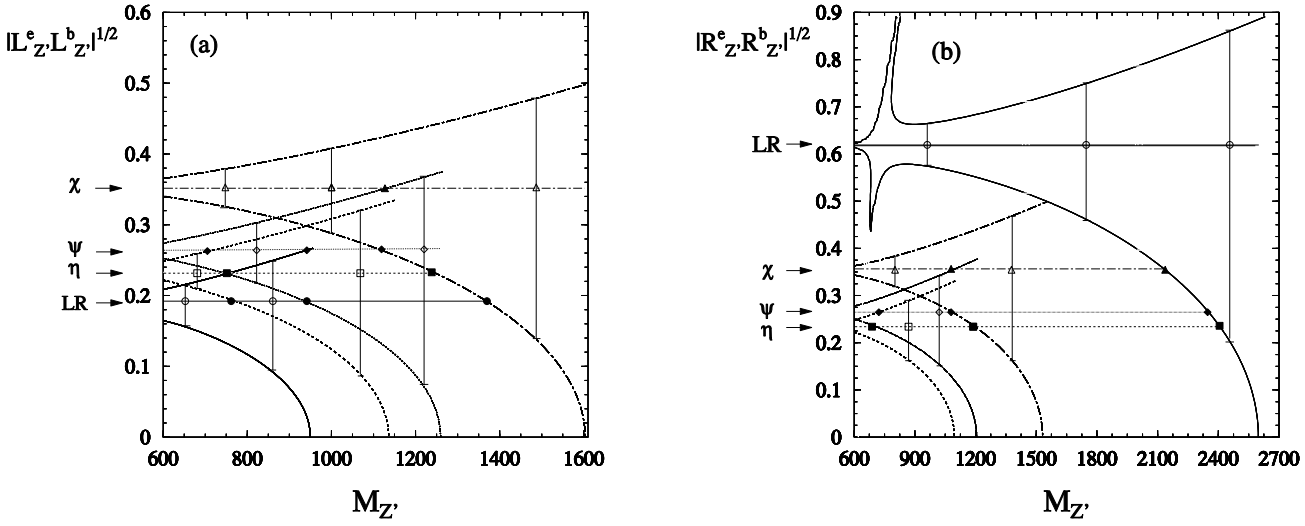

Figure 4: Resolution power at 95% C.L. for $|L^e_{Z'}L^b_{Z'}|^{1/2}$ (a) and $|R^e_{Z'}R^b_{Z'}|^{1/2}$ (b) as a function of $M_{Z'}$ obtained from σ_{LL} and σ_{RR}, respectively, in process $e^+e^- \to \bar{b}b$. The error bars combine statistical and systematic errors. Horizontal lines correspond to the values predicted by typical models.

(with $l = \mu, \tau$ and $q = c, b$). From the numerical point of view, $\sigma_{\alpha\beta}$ are found to just have a complementary role with respect to other observables like σ and $A_{\rm FB}$.

In the case Z' manifestations are observed as deviations from the SM, with $M_{Z'}$ of the order of 1 TeV, the role of $\sigma_{\alpha\beta}$ is more interesting, specially as regards the problem of identifying the various models as potential sources of such non-standard effects. Indeed, in principle, they provide a unique possibility to disentangle and extract numerical values for the chiral couplings of the Z' in a general way (modulo the aforementioned sign ambiguity), avoiding the danger of cancellations, so that Z' model predictions can be tested. Data analyses with other observables may involve combinations of different coupling constants and need some assumption to reduce the number of independent parameters in the χ^2 procedure. In particular, by the analysis combining $\sigma_{\alpha\beta}(l^+l^-)$ and $\sigma_{\alpha\beta}(\bar{q}q)$ one can obtain

information of the Z' couplings with quarks without making assumptions on the values of the leptonic couplings. Numerically, as displayed in the previous Sections,for the class of E_6 and Left-Right models considered here the couplings would be determined to about $3-60\%$ for $M_{Z'} = 1\,\mathrm{TeV}$. Of course, the considerations above hold only in the case where the Z' signal is seen in all observables. Finally, one can notice that for $\sqrt{s} \ll M_{Z'}$ the energy-dependence of the deviations $\Delta\sigma_{\alpha\beta}$ is determined by the SM and that, in particular, the definite sign $\Delta\sigma_{\alpha\alpha}(l^+l^-) < 0$ ($\alpha = L, R$) is typical of the Z'. This property might be helpful in order to identify the Z' as the source of observed deviations from the SM in process (1).

Acknowledgements

It is a pleasure to thank N. Paver for the fruitful and enjoyable collaboration on the topics covered here.

References

[1] Precision Tests of the Standard Electroweak Model, *Advanced Series on Directions in High Energy Physics*, Vol.14, ed. P. Langacker, 1995, World Scientific.

[2] J. Erler and P. Langacker, Phys. Lett. **B 456** (1999) 68.

[3] G. Altarelli, preprint CERN-TH 97-278 (1997).

[4] For a review see, e.g., L. Hewett and T. G. Rizzo, Phys. Rep. **C183** (1989) 193.

[5] A. A. Pankov and N. Paver, Phys. Rev. D **48** (1993) 63.

[6] F. Del Aguila, M. Cvetic and P. Langacker, Phys. Rev. D **52** (1995) 37.

[7] M. Cvetic and S. Godfrey, Summary of the Working Subgroup on Extra Gauge Boson of the DPF long-range planning study, in *Electro-Weak Symmetry Breaking and Beyond the Standard Model*, eds. T. Barklow, S. Dawson, H. Haber and J. Siegrist (World Scientific, Singapore, 1995).

[8] For an extensive review see, e.g., A. Leike, Phys. Rept. **317** (1999) 143.

[9] J.A. Valls, Representing the CDF and D0 Collaborations, Presented at the *QCD and High Energy Interactions, XXXII Rencontres de Moriond*, Les Arcs, March 22-29, 1997, Fermilab report FERMILAB-Conf-97/135-E.

[10] Z' Physics, in *Physics at LEP2*, eds. G. Altarelli, T. Sjöstrand and F. Zwirner, CERN 96-01, Vol.I, p.577.

[11] Contributions to the Workshops e^+e^- *Linear Colliders: Physics and Detector Studies*, ed. by R. Settles, DESY 97–123E.

[12] E. Accomando *et al.*, Phys. Repts. **299** (1998) 1.

[13] P. Osland and A.A. Pankov, Phys. Lett. **B 403** (1997) 93; **B 406** (1997) 328.

[14] A.A. Babich, A.A. Pankov, and N. Paver, Phys. Lett. **B 426** (1998) 375.

[15] A.A. Pankov and N. Paver, Phys. Lett. **B 432** (1998) 159.

[16] A.A. Babich, A.A. Pankov, and N. Paver, Phys. Lett. **B 452** (1999) 355.

[17] G. Altarelli, R. Casalbuoni, D. Dominici, F. Feruglio and R. Gatto, Nucl. Phys. **B 342** (1990) 15.

[18] M. Consoli, W. Hollik and F. Jegerlehner, *in* Z physics at LEP1, ed. G. Altarelli, R. Kleiss and C. Verzegnassi, vol.1, p.7.

[19] S. Riemann, FORTRAN program ZEFIT Version 4.2;
D. Bardin et al., preprint CERN-TH. 6443/92, CERN, 1992.

[20] C. Damerall and D. Jackson, in *Proceedings of the 1996 DPF/DPB Summer Study on New Directions for High Energy Physics - Snowmass96,* Snowmass, CO, 25 June - 12 July, 1996.